Heritage Science

REVIEW

Open Access

Knowledge of earthen heritage deterioration in dry areas of China: salinity effect on the formation of cracked surface crust

Yue Zhang*

Abstract

Numerous important earthen heritage sites in northwestern China have survived until today because of the arid and semi-arid climate. However, most of them suffer from various types and degrees of deterioration, with many questions not answered. Scaling off is one of the main types of deterioration widely observed at the Site of Yar City. To clarify the underlying mechanisms of cracked surface crust formation, previous experimental achievements are reviewed in the framework of unsaturated soil mechanics in this paper. A series of laboratory tests on the properties of local soil during desiccation, including water retention, volumetric shrinkage, cracking and tensile strength, are presented and analyzed, with a particular emphasis on salinity effect. Results show that suction is the key factor controlling the soil behavior. With the decrease in water content, all suction components increased gradually. The presence of NaCl led to a large increase in total suction, but a negligible change in matric suction. The soil shrinkage characteristic curve, which can be divided into three zones, was not affected by NaCl. The suction-loading curve indicates that the change in void ratio was governed by matric suction. In addition, most of the drying shrinkage of soil took place in saturated and near-saturated conditions. According to the quantitative analysis of final crack patterns, the highly fragmented surface morphology tended to be induced in thinner, less salinized soil specimens. The soil tensile strength also increased during drying, which was further enhanced by the cementation of salt crystals between particles. These preliminary results can provide some insights in understanding the on-site deterioration of earthen heritage sites.

Keywords Unsaturated soil, Desiccation, Water retention, Volumetric shrinkage, Cracking, Tensile strength, Deterioration mechanisms

Introduction

As the most original and powerful form of construction, earthen architecture appears globally. According to UNESCO, over 10% of the properties inscribed on the World Heritage List incorporate earthen structures, ranging from simple houses to luxurious palaces, from granaries to religious buildings, and further to historical city centers, cultural landscapes, and archaeological sites [1]. Up to 2019, there were 881 earthen sites out of 5292 National Key Cultural Relics Protection Units throughout China [2]. These sites, with complex building styles and various construction techniques, are deeply rich in historic, artistic, cultural, scientific, and social values [3]. As the physical evidence of ancient societies, they also give a good picture of how human geography, religious beliefs, social economy, military conditions have evolved in different regions.

The existence of earthen sites is affected by natural weathering and human vandalism. Over the past decades, in particular, global climate change, industrialization, urbanization, and so forth, have increasingly

*Correspondence:
Yue Zhang
2019zhangy@shu.edu.cn
Institute for the Conservation of Cultural Heritage, School of Cultural Heritage and Information Management, Shanghai University, Shanghai 200444, China

threatened their long-term preservation. Thanks to the arid and semiarid climate of northwestern China, numerous important earthen heritage sites along the ancient Silk Road have survived to this day. Nevertheless, many previous case studies reported that most remains have undergone different types and degrees of deterioration, with the current situation not being very optimistic [4–10]. Sun et al. [11] established a third-grade classification system for the deterioration of earthen sites, based on the causes, visual manifestation and underlying mechanisms. For deterioration caused by nature, five sub-types are defined, including slice-peeling, recess, cranny, gulch and biological breakage. Li et al. [12] divided the deterioration into four forms, which are property deterioration, structure damaging, structure collapse and site destroying. More specifically, property deterioration includes loosening, fissuring, salinization, and so on. The formation of these features is closely related to the microscopic processes in soil, for example, an increase in porosity, softening of clayey minerals and granular disintegration [13, 14]. Structure damaging is the failure of structural components, typically in the form of mud plaster cracking, holing of walls, foundation problems, etc. In severe cases, structural collapse can be induced to endanger the safety of earthen remains when interacting with gravity stresses and dynamic forces, including strong wind and heavy rainfall [15, 16]. It is worth mentioning that the above-mentioned types of deterioration are regarded as a progressive failure. By contrast, geodynamic processes (earthquakes, floods, and landslides etc.) could have disastrous consequences, even the complete destruction of earthen heritage sites instantaneously [17–20].

The climate of northwestern China is characterized by extreme conditions, including high temperature differences (daily, monthly, and annual), low precipitation with occasional short-lived rainstorms, intense evaporation and strong winds carrying sand [12]. Considering so many influencing factors, revealing the weathering processes of local earthen heritage sites under the condition of multi-scale, multi-field coupling and time sequence combination will lay a scientific foundation for future conservation [2]. Identification of the complex interactions between earthen remains and various environmental parameters has been a hot topic of research for years [9, 10, 12, 21–23]. Field monitoring was performed on rammed earthen walls with an infrared imaging system and temperature sensors in different seasons [24–26]. The changing law of temperature field with respect to time and space was affected by angle and time of solar radiation, orientation of wall, and weathering degree of wall. Within one day, the surface temperature of the wall fluctuated more than that of the surrounding air, the internal temperature of the wall being almost constant. Another important finding is that temperature change is one of the main driving forces for surface weathering. Compared to the nightside, the sunward side of the wall usually experienced greater temperature fluctuations. Consequently, removal of surface crusts from the sunward side of earthen remains was more evident, which might be attributed to the effect of thermal expansion and contraction of soil and the accelerated migration of soluble salts [27, 28]. As for an undercutting area of earthen remains, its formation and development are considered to be governed by two main factors, namely, salinized deterioration and aeolian ullage. Cui et al. [29] conducted real-time monitoring of soil temperature, moisture content and permittivity at three typical sites during concentrated rainfall events. As indicated, the temperature and moisture change over time was very different for the soils in the foundation and in the wall. Such differences facilitated the migration and accumulation of salts towards the undercutting areas. To investigate how the intensity of wind and rain affects deterioration, an on-site experiment was conducted on a test wall at Suoyang Ancient City using specially developed erosion simulation devices [30]. It has been found that compared to clean wind, damage caused by sediment-laden wind was more severe, with features changing from polishing to pitting as the sediment concentration increased. When the wind speed increased, the extent of pitting in terms of area and maximum depth also increased. Wind-driven rain contributes to the cracking and flaking of surface crust. Moreover, it can weaken the cementation between soil particles and then carries the material down the wall face easily. Due to the scouring effect of rainfall, gullies are extensively observed, especially along small fissures and pre-existing channels in earthen walls [31, 32]. Great material loss changes the appearance of earthen remains, and further influences their durability.

Recently, there has been a growing interest in quantitative evaluation of the risk of earthen heritage deterioration. For example, aiming at the Ming Great Wall in Qinghai Province, correlations among soil's engineering properties, deterioration indices, and meteorological factors were preliminarily analyzed [9]. The results show that most cracks, initiating within the joints between rammed plates, are attributed to the construction technology. The plasticity and liquid limit of soil are essential for the emergence of gullies; while the soil salinity, with wind and rainfall, governs the evolution of sapping. Collapse, which directly threatens the stability of earthen remains, is closely related to the evolution of other aforementioned types of deterioration, namely, cracks, gullies and sapping. On this basis, Du et al. [33] adopted Fuzzy-AHP and AHP-TOPSIS methods to obtain vulnerability assessment scores of different earthen sites and compare

their damage levels. Using a newly established Vegetation and Sand TrAnsport model for Heritage Deterioration (ViSTA-HD), Richards et al. [34] linked the environmental processes to the patterns and extent of deterioration found at Suoyang Ancient City. By inputting climatic parameters (e.g., wind velocity, wind flow round vegetation, and sediment transport), the risk of polishing, pitting and slurry on earthen heritage can be simulated over centennial timescales and under multiple different climate scenarios. Through analysis of the environmental temperature and fracture deformation data of the Jiayuguan earthen site, Yu et al. [35] investigated the relationship between these two parameters. Moreover, with the help of support vector machine method, future development of the fracture deformation can be predicted. Obviously, field data provides comprehensive and realistic information on earthen heritage deterioration. However, natural conditions are very complicated and the environmental history of each site since construction is generally unknown. Similar deterioration features might result from different erosion effects; in other cases, a specific weathering process leads to either the formation of new features or the development or erosion of existing features [10].

Therefore, to clarify the underlying mechanisms of deterioration with respect to each environmental factor, it is also essential to perform delicate laboratory tests on soil samples under strictly controlled conditions. Regarding earthen heritage sites in northwestern China, many contributions have been made to reveal the individual or synthetical influences of temperature, water and soluble salts, from both macro and micro perspectives [36–44]. Drying-wetting and freezing–thawing cycles were mainly conducted and changes in soil properties were assessed, such as mass, surface roughness, surface hardness, ultrasonic pulse velocity, mechanical strength and porosity. During this process, the wind erosion rate and disintegrating speed were found to increase, indicating an obvious reduction in the weathering resistance of soil [45–48]. Some researchers also focused on the thermal parameters (thermal conductivity coefficient, thermal diffusion coefficient, specific heat of volume) [49, 50] and deformation characteristics of heritage soils [51]. In fact, these physical parameters play a key role in causing fatigue failure, especially for multi-layer structures such as wall-paintings and crusted walls. Due to the different parameters of the two layers, interface stresses can be generated, resulting in a detachment of surface layer. In recent years, a growing number of papers have focused on the salt-induced deterioration of earthen heritage in northwestern China. The research includes two main aspects: (1) migration and distribution of salts [44, 52–58], and (2) dynamic processes and mechanisms of destruction [40, 46, 59–64]. As reported, factors including soil properties, types and content of soluble salts and environmental conditions operate together, which govern the position and characteristics of deterioration occurring at earthen sites.

Soils near to the ground surface in dry areas are generally unsaturated and their pores are filled partly with liquid water and partly with air. In addition to solids, air, and water, the fourth independent phase exists, called the contractile skin or the air–water interface. It acts like a thin, elastic membrane interwoven throughout the voids of soil, pulling the particles together through surface tension. As a result, the position of the contractile skin, which is dependent on the water degree of saturation, has a great impact on the mechanical and hydraulic properties of an unsaturated soil [65, 66]. Some Chinese researchers have studied the soil–water characteristics and unsaturated hydraulic conductivity of earthen plaster in the murals of Mogao Grottoes, considering the effects of soil compositions, salts, and environmental humidity [67–70]. Zhang et al. [36] discussed the influence of drying-wetting cycles on the durability of heritage soil from the perspective of unsaturated soil mechanics. In fact, the repeated action of air–water interface on soil particles leads to the fatigue failure of the structure.

Significant progress has been made in previous studies to promote understanding of the deterioration of earthen heritage sites in China's dry areas. However, many questions remain to be clarified regarding the formation and development of various deterioration features. Investigation into the overall behavior of heritage soils, especially under a multi-field coupling condition, is also required. In this paper, a famous earthen heritage site in northwestern China, namely, the Site of Yar City, with its current state of deterioration is introduced. Based on a literature review, previous experimental achievements on the formation of cracked surface crust are presented. The effect of salinity on the properties of local heritage soil, including water retention, volumetric shrinkage, cracking and tensile strength, is analyzed using unsaturated soil mechanics as a tool. Finally, the implication of laboratory work for understanding on-site deterioration is discussed and some key issues are proposed for future research.

Research framework

Study site

General background

The Site of Yar City, also known as the Ancient City of Jiaohe, is located in the western Turpan Basin in the Xinjiang Uygur Autonomous Region of China. The city was built more than 2000 years ago and became the capital of the South Cheshi State, which was one of the kingdoms of the Han dynasty. Throughout history, different

ethnic groups have lived here, enhancing the harmonious coexistence and integration of diverse cultures. As a gateway between the East and the West, Yar City had exerted considerable political, economic and military influence on surrounding regions and reached its golden age in the Tang dynasty. Precisely because of its important traffic and geo-strategic location along the Silk Road, Yar City suffered from successive wars in the late Yuan dynasty, resulting in severe destruction and permanent abandonment.

Most of the structures that remain at the site today date from the Tang dynasty. Despite many centuries have passed, Buddhist temples, government offices, folk houses, streets, handicraft workshops, city gates, watchtowers, tombs and so on can be clearly distinguished. Various building techniques were used in combination, including raw soil, rammed earth, adobe masonry and mud piled construction, fully demonstrating the diversity and uniqueness of architectural styles [3]. This earthen site was listed as a National Key Cultural Relics Protection Unit and World Heritage site in 1961 and 2014, respectively.

The Site of Yar City lies on a loess plateau at the Yarnaiz Groove village, atop a cliff over 30 m in the WN-ES direction (Fig. 1a). This tableland has a shape of willow leaf and its longest length from north to south is 1787 m and the widest width from west to east is around 310 m [71]. Geological information from the borehole shows that this area contains a wide spread of Quaternary sediments. Soil near the surface (with a thickness of about 25–26 m) is dominated by interlayers of silt, silty clay, and fine sand, whose particle size increases gradually with increasing depth [72].

The Turpan Basin, one of the most arid regions in China and even in the world, is a typical closed inland basin surrounded by high mountains. Such location, topography and terrain conditions contribute to its unique temperate arid desert climate, that is dry, hot and windy. Statistical data obtained from weather stations of Turpan, Tockson and Shanshan show that the minimum and maximum average monthly temperatures were − 15.9 ℃ (in January) and 34.1 ℃ (in July), respectively [73]. Historically, the extremely high temperatures in the Site of Yar City have reached almost 50 ℃ for air and 82.3 ℃ for the soil surface [74]. In addition, the average annual precipitation in the basin is only 16.6 mm; whereas the average annual evaporation is above 2500 mm. Nearly half of the precipitation is concentrated during the summer season (from June to August).

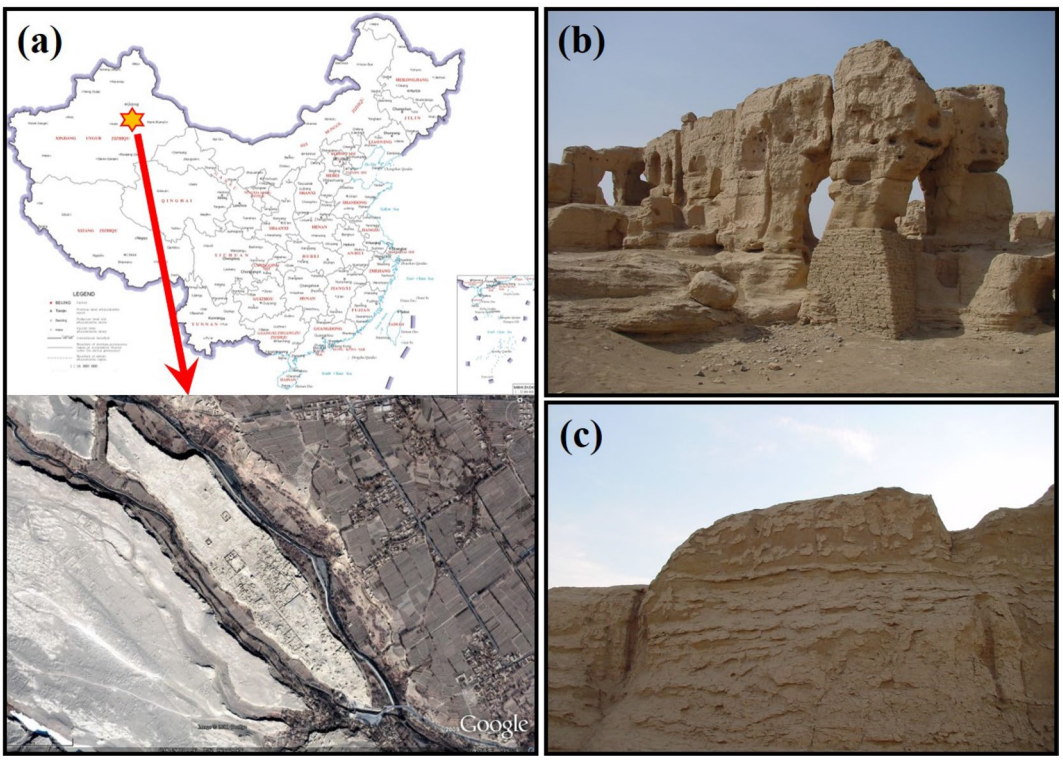

Fig. 1 The Site of Yar City. **a** Its location and satellite image (from Google Maps); **b** The remains suffering from complicated damages; **c** The detachment of cracked surface crusts

Current state of deterioration

The Site of Yar City is considered to be the oldest, largest and best-preserved earthen site in the present world. However, it also suffers from a series of complicated damages, such as surface erosion, gullies, cracks and collapse [22, 71, 75] (Fig. 1b). Among all types of deterioration, scaling off is the most common and typical, which distributes extensively on earthen remains (Fig. 1c). Field studies reveal that scaling off has a binary structure [28, 76, 77]. Its planar form is crusted soil cut by cracks, while some pieces have lifted edges. The profile of scaling off is characterized by obvious stratification, with another loose soil layer underneath the surface crust. There is also a large amount of white crystalline substances aggregated on the second layer.

Surface crust formation is associated with the occasional but heavy rainstorms in northwestern China [22, 27]. More specifically, soil materials on the surface of earthen walls can be disintegrated and removed by the strikes of raindrops. When the dispersed soil particles enter the wall with rainwater, the pore structure becomes clogged. This will further promote the soil saturation and the formation of flowing slurry on wall surfaces. During the subsequent intense evaporation, the slurry dries up and shrinks gradually, turning into a layer of hard but cracked surface crust. In the Site of Yar City, the thickness of surface crust has been found to vary between approximately 1–15 mm, depending on the construction techniques [27]. As the original integrity of the wall surface is destroyed by cracks, gaseous and liquid substances can penetrate deeper into the wall through preferential flow paths. Consequently, surface crusts are easily removed by wind deflation and sand abrasion. Over the years, scaling off has thinned and lowered earthen remains, substantially accelerating the progressive destruction and extinction of heritage sites. Moreover, soluble salts such as NaCl are concentrated in walls, especially in the capillary zone. The total salt content is generally in the range of 2–6%, which is significantly higher than that of the foundation soil (< 0.7%).

Experimental program

Materials

With the intention of not causing destruction of earthen remains, the tested soil was acquired from the ground surface at the Site of Yar City. After crushing and sifting through a 2 mm sieve, the soil powder was completely dried at 105 °C. The mineralogical composition and particle size distribution were determined using an X-ray diffractometer and a laser particle size analyzer, respectively. The basic characteristics of the soil are listed in Table 1. As can be seen, the soil was dominated by silt particles, which can be classified as low plasticity clay.

Table 1 The basic characteristics of the soil material in the Site of Yar City

Soil properties	Values	
	[78]	[79]
Specific gravity	2.700	2.719
Consistency limits (%)		
LL	30.0	34.0
PL	19.0	22.4
Main minerals (%)		
Quartz	55.0	39.2
Albite	16.0	34.9
Orthoclase	10.0	18.3
Clinochlore	9.0	
Calcite	8.0	
Montmorillonite		2.3
Illite		2.1
Kaolinite		2.0
Particle size distribution (%)		
Sand	4.4	7.5
Silt	79.4	67.4
Clay	16.2	25.1

Chemical analyses indicated that the major cations and anions present in the pore water were Na^+, K^+, Ca^{2+}, Cl^-, SO_4^{2-}, and NO_3^- [78].

To reproduce the process of surface crust formation on salt-laden earthen walls, slurry specimens with different salinity levels were prepared. The detailed steps include: (1) soil desalinization and oven-drying, (2) thorough mixing of the soil with distilled water and salt, and (3) sealing and equilibration of slurry [78]. Note that the effect of desalinization was assessed by measuring the electrical conductivity of solution extracted from the soil. The initial water content of slurry specimens was 45% (1.5 times the liquid limit), with consideration of three different mass contents of NaCl (0, 2, and 5%). After equilibration, the obtained slurry had a homogeneous initial dry density of 1.25 Mg/m^3 and a good consistency for handling.

Methods

The research mainly focused on the evolution of soil properties during desiccation. Table 2 summarizes the laboratory tests, all of which were conducted in air-conditioned room at an ambient temperature of 20 ± 1 °C.

- Water retention property. The water retention curve (WRC), or the soil–water characteristics curve (SWCC), is fundamental and indispensable for interpreting the behavior of unsaturated soils. It defines the amount of water in a soil versus soil suctions. Various

Table 2 A summary of laboratory tests

Soil properties	Laboratory tests		
	Specimen	Methods	References
Water retention	Circular	Pressure plate, high-capacity tensiometer, water potentiometer, vapor equilibrium, and filter paper	[80, 81]
Volumetric shrinkage	Circular	Fluid displacement	[80, 82]
Cracking	Square	Digital image processing and analysis	[78]
Tensile strength	Cylindrical	Uniaxial tensile loading	[83]

direct or indirect techniques are available to control or measure soil suction in the laboratory [84]. Here, five common methods were adopted in combination, i.e., pressure plate, high-capacity tensiometer, water potentiometer, vapor equilibrium, and filter paper, according to international standards.

- Volumetric shrinkage property. Drying shrinkage is ubiquitous, especially in fine-grained soils. The soil shrinkage characteristic curve (SSCC) is a graphical representation of void ratio versus water content. For slurry specimens dried under an unconstrained condition, change in the volume was measured indirectly using the fluid displacement method.
- Cracking property. Once the drying shrinkage of a soil is restrained, cracking tends to occur to induce fragmentation. Different amounts of slurries were poured into rectangular glass containers, forming specimens with initial layer thickness of 2.4 mm and 4.8 mm, respectively. Then, the weight was constantly monitored and the surface morphology was recorded using a Nikon D80 digital camera. The obtained images were then processed with the Crack Image Analysis System (CIAS) software [85] for quantitative analysis.
- Tensile strength property. Desiccation cracking is in fact a form of damage induced by stress. An increase in suction contributes to the accumulation of effective stress in soil skeleton. When such internal stresses exceed the tensile strength of soil, cracks begin to form and propagate. Using a specially designed apparatus, uniaxial tensile tests were conducted on specimens with different water contents dried from soil slurry. The tensile load was applied directly to both ends of a specimen at a constant displacement rate (0.5 mm/min). The axial load and the displacement were continuously recorded to obtain the tensile strength of soil.

Properties of heritage soil

Water retention

The evolution of water content of the slurry specimens with respect to matric suction obtained by pressure plate method is shown in Fig. 2a. As the matric suction increased from 0 to 1100 kPa, a gradual decrease in water content was induced from its initial value of 45% to about 11.5%. However, there was no significant discrepancy among specimens with different NaCl contents. In fact, in pressure plate, the matric suction of the soil was strictly controlled by applying a specific difference between the pressures of pore air and pore water. Figure 2b indicates that for the NaCl-free specimen, data obtained using high-capacity tensiometer and filter paper (contact) were comparable to those obtained by pressure plate. It should be noted that, for pressure plate and high-capacity tensiometer methods, the upper limit of matric suction is governed by the air-entry value of the ceramic stone adopted, which is generally not more than 1500 kPa. In comparison, filter paper method applies to almost the full range of soil suction.

WRCs measured on the heritage soil in terms of total suction are presented in Fig. 2c. With the increase in NaCl content, the total suction increased by several orders of magnitude, especially at a relatively high water content. When the specimens became drier, the total suction also increased continuously. Once the water content dropped below 3%, with further drying, the total suction values of all specimens tended to become close. The results of the NaCl-free specimen indicate that, compared to filter paper (non-contact) and vapor equilibrium methods, the total suctions measured by water potentiometer were larger. This phenomenon can be explained by different testing periods. More specifically, to measure total suction indirectly, soil needs to reach moisture equilibrium with the environment in an enclosed space. Measurements by water potentiometer method took only a few minutes, whereas non-contact filter paper and vapor equilibrium methods usually lasted several weeks or even months. Therefore, discrepancies among the data of different methods could not possibly be overlooked, particularly in the lower range of total suction.

Because of the presence of NaCl in soil specimens, a difference was induced between the total suction and matric suction at a specific water content, known as osmotic suction. Obviously, the higher the NaCl content,

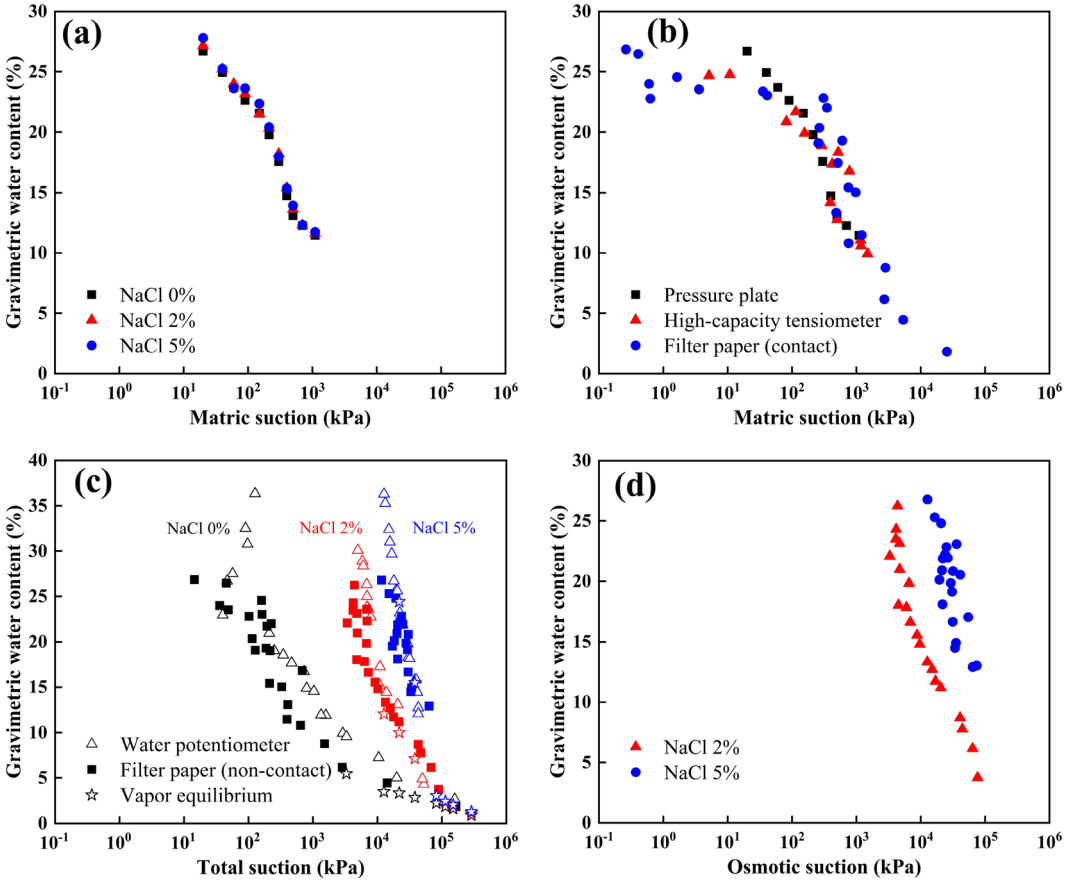

Fig. 2 WRCs of the heritage soil [80, 81]. **a** Water content versus matric suction obtained by pressure plate method; **b** Water content versus matric suction obtained on NaCl-free specimen by different methods; **c** Water content versus total suction obtained by different methods; **d** Water content versus osmotic suction of NaCl-contaminated specimens

the larger the osmotic suction (Fig. 2d). Additionally, osmotic suction increased gradually with continuous drying, rather than remaining constant. This is because the concentration of pore fluid in soil specimens continued to increase throughout the desiccation process.

Volumetric shrinkage

It is clear that along the drying path, the SSCC obtained can be divided sequentially into three parts including proportional, residual and zero shrinkage zones (Fig. 3a). This is a typical shape of SSCC for clay paste or slurry in which the bond between particles is weak and no aggregates and macropores exist [86]. As can be seen, at first, the void ratio decreased linearly with the water content. Since the reduction in bulk volume of soil was totally equal to the amount of water that evaporated, the specimens remained fully saturated ($S = 100\%$). When the water content continued to decrease, the residual shrinkage zone was reached in which soil deformation occurred continuously, but at a decreasing rate. During this process, the air has progressively entered the pores and the soil became unsaturated. In the zero shrinkage zone, the void ratio of soil eventually stopped decreasing with further moisture loss and reached a residual value of about 0.54. Note that the water content values corresponding to the transition points of different zones on SSCC are important indicators of the drying shrinkage behavior of soil. In this case, water content of 22% and 16% was regarded as the air-entry water content (W_{AE}) and the shrinkage limit (W_{SL}) of the heritage soil, respectively.

When the soil is desiccated under zero net confining pressure, suction, also known as hydraulic stress, is the dominant contributor to deformation. The suction-loading curve, which illustrates the relationship between void ratio and suction, is essential for characterizing the consolidation process [87]. In fact, the SSCCs of the heritage soil in Fig. 3a indicate that the osmotic suction related to the presence of NaCl had a negligible impact on its volumetric shrinkage behavior. Therefore, void ratio can be plotted against matric suction by combining the SSCC of the NaCl-free specimen with its WRC.

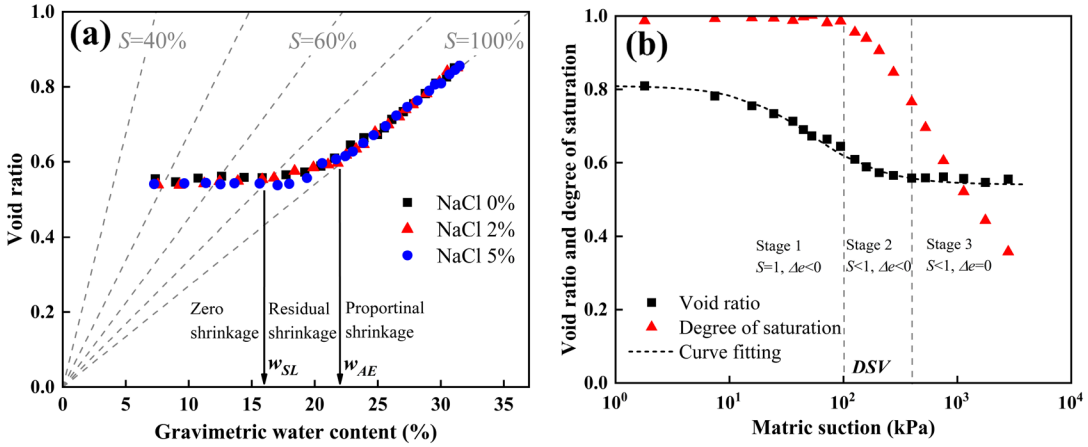

Fig. 3 **a** SSCCs of the heritage soil; **b** Void ratio and degree of saturation versus matric suction of NaCl-free specimen [80]

As shown in Fig. 3b, when the matric suction was below 10 kPa, its effect on soil particle rearrangement was so small that no obvious change in void ratio was observed. With an increase in the matric suction, soil particles gradually approached and contacted each other, resulting in a remarkable reduction in the void ratio. At a matric suction of approximately 400 kPa, the densest soil structure was formed. The suction-loading curve of the heritage soil can be well fitted by the following model [88]:

$$e = e_r + \frac{e_s - e_r}{1 + A\psi_m^B} \tag{1}$$

where ψ_m is the matric suction; e_s and e_r are the initial and final void ratio of the curve, respectively; A and B are model parameters to be determined.

Variation in the degree of saturation is also presented in Fig. 3b. It shows that the heritage soil began to desaturate at about 100 kPa, which is therefore defined as the desaturation value (DSV). When the volumetric deformation of soil specimen became stable, the degree of saturation was still relatively high ($S \approx 0.8$). Obviously, most of the drying shrinkage took place in saturated and near-saturated conditions. A similar trend has also been reported on soil slurries by other researchers [89, 90].

Cracking

The test results show that, for all specimens, the desiccation process exhibited a similar pattern, namely that the water content decreased rapidly and linearly with drying time at the beginning (Fig. 4). Thereafter, there was an obvious slowdown in evaporation rate until the water content became constant. The time it took for the heritage soil to reach final stabilization increased considerably with increasing NaCl content and layer thickness.

At the end of desiccation, specimens with higher NaCl content were visually darker due to the higher residual water content (Fig. 5). In addition, the surface morphology of soil was significantly influenced by layer thickness. By comparison, specimens of a smaller thickness (2.4 mm) were extensively cut by narrower cracks into many smaller segments. In Fig. 6, the black and white binary images of specimens containing 2% NaCl reveal the evolution of crack networks during desiccation. It is clear that for both specimens, cracking started from the edges, which then stabilized when the water content was close to the air-entry water content (22%). This phenomenon is well consistent with the aforementioned volumetric shrinkage results: most of the drying deformation of the tested soil slurries occurred when saturated. However, the cracks in the thin specimens mainly originated at one point and propagated simultaneously in three

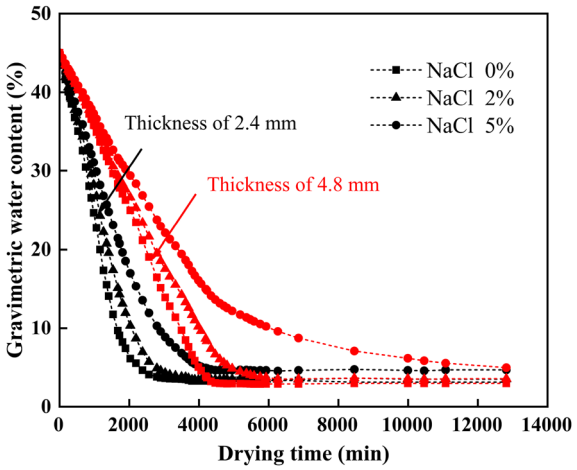

Fig. 4 Evolution of water content with drying time of the heritage soil [78]

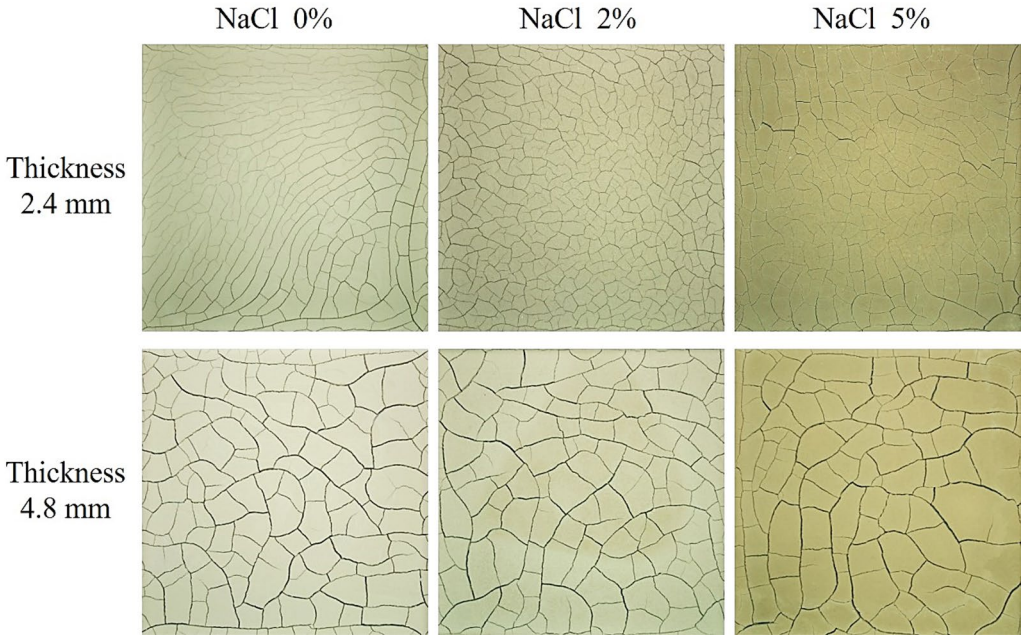

Fig. 5 Surface morphology of the heritage soil at the end of desiccation [78]

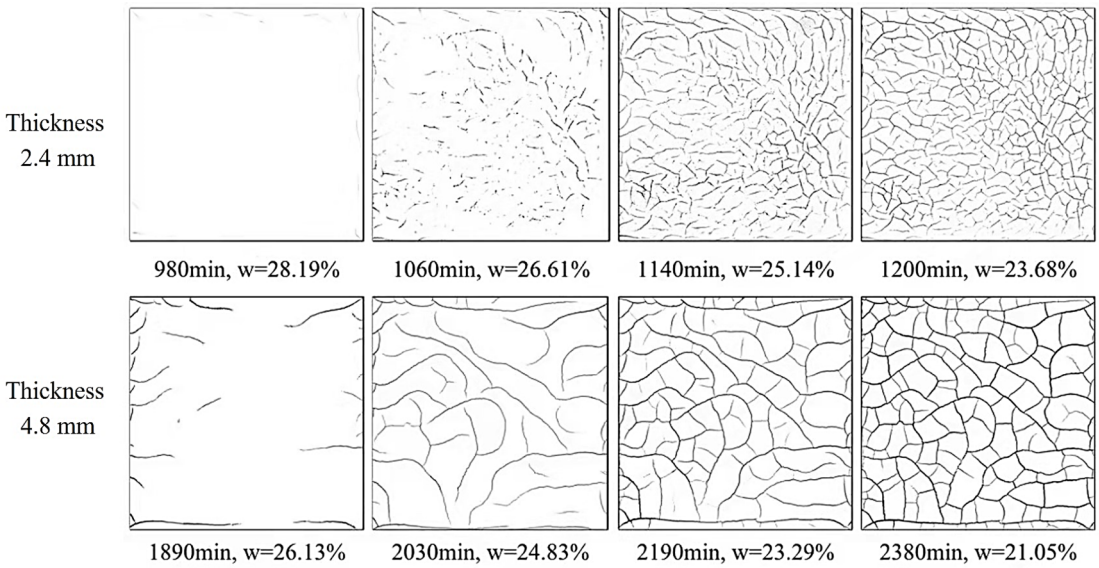

Fig. 6 Evolution of crack network in specimens containing 2% NaCl [78]

directions with intersection angles of roughly 120°, forming a non-orthogonal cracking pattern. In the thick specimens, the cracks developed sequentially and met at right angles, which induced an orthogonal crack pattern.

The final crack patterns were described quantitatively in terms of crack intensity factor (CIF), intersection number, segment number and total crack length. As listed in Table 3, all the geometric parameters decreased as the NaCl content increased. The NaCl-free specimen of 2.4 mm thickness was an exception because many surface cracks developed insufficiently, resulting in a deviation in the software analysis. With increasing layer thickness, the CIF increased while other parameters decreased. The data generally confirmed that drying cracks tended to produce a highly fragmented surface in thinner soil specimens.

Table 3 Quantitative analysis of the final crack patterns [78]

Specimens		Geometric parameters			
Thickness	NaCl content	CIF	Intersection number	Segment number	Total crack length
2.4 mm	0%	7.15%	325	188	58,091
	2%	6.25%	602	332	68,943
	5%	5.06%	338	188	49,608
4.8 mm	0%	8.78%	235	169	41,170
	2%	6.38%	210	143	38,949
	5%	6.36%	175	116	34,671

Tensile strength

The results of the uniaxial tensile tests are presented in Fig. 7a. In the studied range, tensile strength of the heritage soil increased during desiccation, which exhibited an approximate linear relationship with the water content. Additionally, the impact of NaCl is obvious that under the same moisture conditions, specimens with more NaCl tended to have a higher tensile strength value. This can be explained by the precipitation of salt crystals from the pore fluid that filled the voids and increased the cementation between soil particles [91]. As illustrated in Fig. 7b, higher tensile strength was measured at higher matric suction. Aiming at the heritage soil obtained also from the Site of Yar City, Liu [92] conducted the unconfined

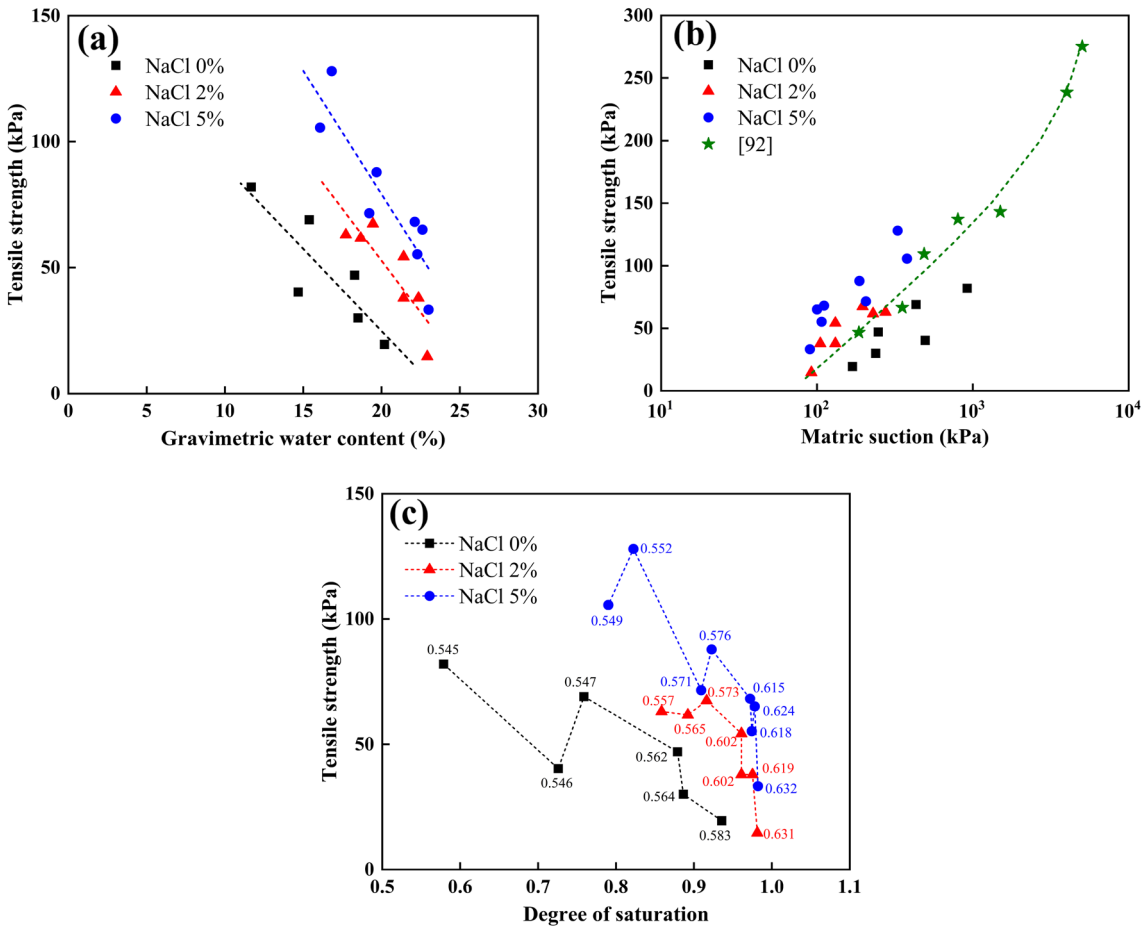

Fig. 7 Evolution of tensile strength of the heritage soil [83]. **a** Tensile strength versus water content; **b** Tensile strength versus matric suction; **c** Tensile strength versus degree of saturation

penetration test to determine its tensile strength. Despite the difference in the soil composition and testing methods of two studies, the variation in tensile strength with respect to matric suction was generally similar.

Figure 7c presents the relationship between the tensile strength and the degree of saturation, with void ratios given as labels. It is clear that tensile strength of the heritage soil increased gradually with the decrease in degree of saturation. As stated previously, at higher degree of saturation (water content), great volumetric shrinkage of soil can be caused by increased matric suction. Consequently, the contact areas between particles increased to attain a higher tensile strength, even if the specimen was still saturated. Similar findings have also been reported in previous research [93].

Implication for on-site deterioration

The initial characteristics of earthen remains in various heritage sites are generally quite different (Fig. 8). Intrinsic factors of a soil such as the composition and microstructure are critical to how it behaves during subsequent events.

When subjected to rainfall, soil aggregates on a wall surface can be disrupted into smaller ones by two effects: the slaking due to wetting and the mechanical breakdown due to hammering of falling raindrops. The rate of breakdown is dependent on the erodibility of soil (i.e., aggregate stability) and the erosivity of rain (i.e., rainfall intensity and duration). It has been found that the aggregate stability increases with the content of soil cements such as clay and organic matter [94]. It is also affected by the antecedent water content of soil [95]. As mentioned earlier, annual precipitation in northwestern China is very low, but short-lived and heavy rainstorms are common, especially in summer seasons. Rapid soil wetting occurs at higher rainfall intensities [94]. In this case, a greater loss of aggregate stability is induced by the slaking effect; a higher air pressure is also created within the pores to further promote the breakdown of aggregates. As a result, most surface and subsurface soil aggregates are destroyed by rain drops, which improves the sealing and clogging of pores and the reduction of water infiltration into the soil [96, 97]. When the rainfall intensity exceeds the infiltration rate, runoff occurs on the surface of the earthen remains to form a slurry.

In the subsequent evaporation process, the drying rate of a flowing slurry is governed by factors such as air temperature, relative humidity, solar radiation and airflow. For different drying rates, variation in the degree of saturation and void ratio of a soil with respect to elapsed time can be very different, whereas the SSCC was unaffected [98]. This means that for a specific type of soil dried under zero net confining pressure, its void ratio is a unique function of matric suction. However, previous studies show that evolution of the crack network in a drying soil is a process correlated simultaneously

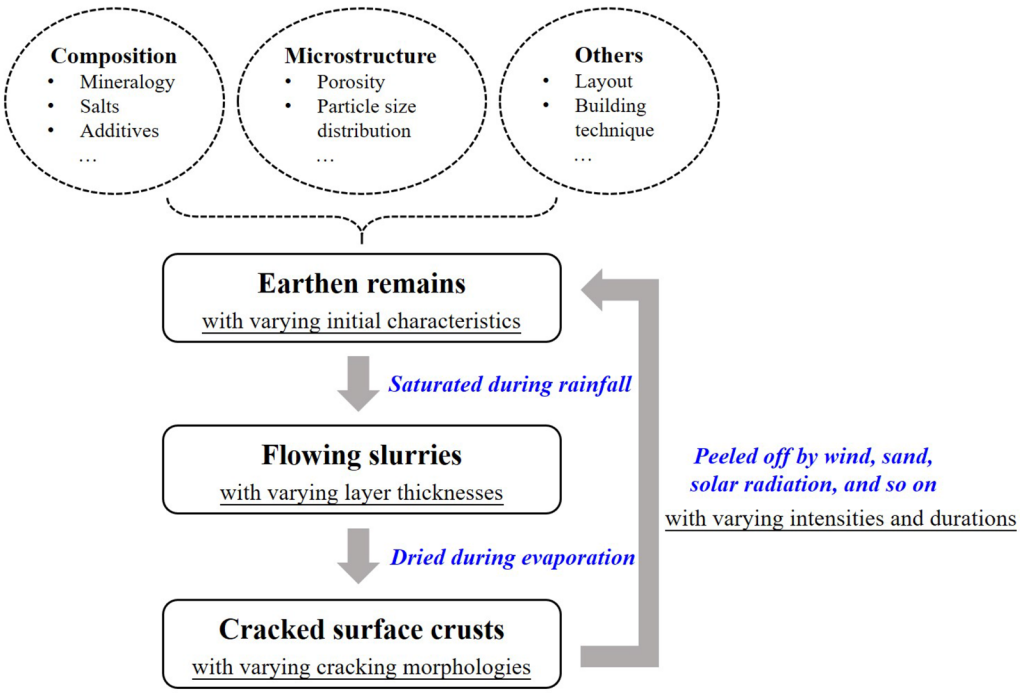

Fig. 8 Schematic illustration of the deterioration mechanisms of cracked surface crusts in earthen heritage sites

with water evaporation, suction change and volumetric shrinkage. The dynamics and morphology of cracking depend largely on the environmental conditions, boundary constraints, and so on [99]. For example, the severity of cracking, which is characterized by the number of segments formed, increases with increasing temperature, but with decreasing air humidity [100]. The geometric parameters of a crack pattern also vary as the surface area of a soil specimen changes. Therefore, the size effect should be carefully considered when upscaling experimental results from the laboratory to the field and vice versa [101].

Removal of surface crusts by a clean wind is attributed to the effect of shear stress, which can be further exacerbated if the wind is laden with sediments. The greater the wind velocity, the greater the number and kinetic energy of sand particles in the wind-sand flow. The striking and abrasive motion of the sand particles makes the soil grains come loose and fall constantly from the parent material. The detachment of surface crusts is widely distributed not only on the windward walls, but also on the west- and south-facing walls that are exposed to intense solar radiation and temperature fluctuations [27]. Also, as the level of drought increases, the degree of scaling off of earthen sites becomes more severe [77]. In comparison with collapse, scaling off has been regarded as the least significant type of deterioration of earthen heritage, as it is neither highly correlated with other types of deterioration nor threatening the structural stability. However, the accumulative material loss resulting from the cyclic formation and detachment of the surface crusts cannot be ignored, especially in the long run. Faced with considerable uncertainty regarding the future climate change, both locally and globally, more attention needs to be paid to the earthen heritage deterioration in dry areas of China.

Conclusions

Earthen remains in heritage sites in dry areas of China are subjected to various types and degrees of deterioration. Many contributions have already been made to identify the influences of environmental factors on soil materials and assess the risk of deterioration, both in the laboratory and in the field. However, the behavior of heritage soils, especially in multi-field coupling conditions, remains uncertain.

Cracked surface crusts are widely distributed in the Site of Yar City, a famous earthen heritage site in northwestern China. To reveal the underlying deterioration mechanisms, previous researches are systematically reviewed and discussed in this paper in the framework of unsaturated soil mechanics. The salinity effect on soil properties, including water retention, volumetric shrinkage, cracking and tensile strength, are mainly evaluated.

The results indicate that all the suction components increased gradually as water content decreased. The total suction was increased significantly by adding NaCl, while the matric suction was hardly influenced. The impact of NaCl on SSCCs of heritage soil was also negligible. Variation in NaCl content and layer thickness induced changes in the final crack patterns. Quantitative analysis by geometric parameters shows that highly fragmented surface morphology was formed in thinner, less salinized soil specimens. In addition, tensile strength of the heritage soil was enhanced by both matric suction and NaCl, which increased the contact areas and cementation between soil particles.

Even today, deterioration of earthen heritage sites in dry areas of China continues and will never stop. Due to the long-term unsaturated state of these remains, application of unsaturated soil mechanics provides additional information. Suction and water retention curve are basic and essential for quantitatively describing the soil properties. There is no doubt that laboratory experiments can help establish a reliable database for analysis under water-salt coupling conditions. However, the real conditions in the natural environment are so complicated that more coupling factors should be considered. Moreover, effort should also be devoted to the field investigation on relevant issues.

Acknowledgements
Not applicable.

Author contributions
YZ wrote and revised the manuscript. The author read and approved the final manuscript.

Funding
This work was supported by the National Natural Science Foundation of China (42007265).

Availability of data and materials
Not applicable.

Declarations

Competing interests
The authors declare that they have no competing interests.

Received: 21 November 2022 Accepted: 21 February 2023
Published online: 28 February 2023

References

1. WHEAP. World Heritage Inventory of Earthen Architecture. UNESCO; 2012. http://whc.unesco.org/en/news/879. Accessed 5 Oct 2022.
2. Guo QL, Wang YW, Chen WW, Pei QQ, Sun ML, Yang SL, Zhang JK, Du YM. Key issues and research progress on the deterioration processes and protection technology of earthen sites under multi-field coupling. Coatings. 2022;12:1677.

3. Pei QQ, Guo QL, Wang XD, Zhao JZ, Zhao GJ, Luo J. Evolution and characteristics of traditional building techniques for earthen architectural sites. Sci Conserv Archaeol. 2019;31(5):1–13 (**in Chinese**).
4. Wang XD, Zhang L, Li ZX, Wang CF, Li WT. The study of existing condition and consolidation project of No. 3 tomb of the western Xia Mauseoleums. Dunhuang Res. 2002;4:64–72112 (**in Chinese**).
5. Zhao HY, Li ZX, Han WF, Sun ML, Wang XD. Study on the main disease of the Great Wall and its conservation in Gansu province. Sci Conserv Archaeol. 2007;19(1):28–32 (**in Chinese**).
6. Li ZX, Zhao LY, Sun ML. Deterioration of earthen sites and consolidation with PS material along Silk Road of China. Chin J Rock Mechan Eng. 2009;28(5):1047–54 (**in Chinese**).
7. Huang SP, Li YH, Xiao YP, Jin PJ, Wang S. Studies on the prevention and control of biological damage in Tang Hanguang entrance remains. Sci Conserv Archaeol. 2010;22(2):6–11 (**in Chinese**).
8. Zhang GW, Zhang HY, Yu ZR. On the deterioration of and consolidation measures for Ancient Andier City in Xinjiang. Dunhuang Res. 2014;5:125–30 (**in Chinese**).
9. Du YM, Chen WW, Cui K, Gong SY, Pu TB, Fu XL. A model characterizing deterioration at earthen sites of the Ming Great Wall in Qinghai Province. China Soil Mech Found Eng. 2017;53(6):426–34.
10. Richards J, Viles H, Guo QL. The importance of wind as a driver of earthen heritage deterioration in dryland environments. Geomorphology. 2020;369:107363.
11. Sun ML, Li ZX, Wang XD, Chen WW. Classification of deteriorations associated with many earthen heritage sites in arid areas of northwest China. J Eng Geol. 2007;15(6):772–8 (**in Chinese**).
12. Li L, Shao MS, Wang SJ, Li ZX. Preservation of earthen heritage sites on the silk road, northwest China from the impact of the environment. Environ Earth Sci. 2011;64(6):1625–39.
13. Yang L, Zhang HY, Liu P, Wang PT, Tan Y. Microcosmic study on superficial layer diseases in rammed earthen ruins of great wall in arid area. J Arid Land Resour Environ. 2017;31(11):75–80 (**in Chinese**).
14. Chen Y, Zhang HY, Yang L. Analogy study on evolution of microstructure of earthen monument during natural weathering process. Rock Soil Mech. 2018;39(11):4117–24 (**in Chinese**).
15. Zhao D, Tu BB, Wang YL. Analysis of structure defect of shikchin ground Buddhist Temple site. Chin J Geol Hazard Control. 2013;24(2):111–5 (**in Chinese**).
16. Ding ZH, Wu GZ, Liu Y. Research on the structural stability diseases and traditional conservation methods for the great wall made of rammed earth. Geotech Investig Surv. 2020;48(6):24–32 (**in Chinese**).
17. Wang XD, Shi YC, Liu K. Research on sapping instability mechanism for rammed wall. Northwestern Seismol J. 2011;33:381–5 (**in Chinese**).
18. Guo ZQ, Chen WW. Dynamic responses of single earthen sites under seismic loads: a case study of the Liufuzhai Watchtower in Shandan China. China Earthquake Eng J. 2017;39(4):609–16 (**in Chinese**).
19. Kong DZ, Shi YC, Liang QG, Lu YX. Dynamic response analysis and seismic stability of the rammed Great Wall of different types under earthquake action. J Seismol Res. 2018;41(2):328–36 (**in Chinese**).
20. Zhang HY, Zhu F, Kou KH, Liang Z. Historical and present situation of the flood control at the Luotuo City Site in Gaotai. Gansu Province Dunhuang Res. 2019;1:133–40 (**in Chinese**).
21. Cui K, Chen WW, Han L, Wang XD, Han WF. Effects of salinized deterioration and aeolian ullage on soils in undercutting area of earthen ruins in arid region. Chin J Geotech Eng. 2011;33(9):1412–8 (**in Chinese**).
22. Shao MS, Li L, Wang SJ, Wang EZ, Li ZX. Deterioration mechanisms of building materials of Jiaohe ruins in China. J Cult Herit. 2013;14(1):38–44.
23. Richards J, Bailey R, Mayaud J, Viles H, Guo QL, Wang XD. Deterioration risk of dryland earthen heritage sites facing future climatic uncertainty. Sci Rep. 2020;10:16419.
24. Zheng L, Zhou ZH, Zhang HY, Sun B, Bai L. Monitoring the temperature changes of earthen architecture walls. J Lanzhou Univ (Natural Sciences). 2008;44(supp):58–60 (**in Chinese**).
25. Sun B, Zhou ZH, Zhang HY, Zhang YX, Zheng L. Characteristics and prediction model of surface temperature for rammed earthen architecture ruins. Rock and Soil Mech. 2011;32(3):867–71 (**in Chinese**).
26. Pei QQ, Zhang B, Shang DJ, Guo QL, Huang JJ, Zhu J. Characteristics of temperature field of rammed earth wall in arid environment. Coatings. 2022;12:735.
27. Zhang HY, Liu P, Wang JF, Wang XD. Generation and detachment of surface crust on ancient earthen architectures. Rock and Soil Mech. 2009;30(7):1883–91 (**in Chinese**).
28. Du YM, Cui K, Chen SY, Dong WQ, Chen WW. Quantitative research on the development difference of scaling off on the sunward side and nightside of earthen sites. J Cult Herit. 2022;57:107–17.
29. Cui K, Guan XP, Chen WW, Chen MM, Han WF. Effects of salinized deterioration and aeolian ullage on soils in undercutting area of earthen ruins in arid regions (II). Chin J Geotech Eng. 2017;39(10):1777–84 (**in Chinese**).
30. Richards J, Zhao G, Zhang H, Viles H. A controlled field experiment to investigate the deterioration of earthen heritage by wind and rain. Heritage Sci. 2019;7:51.
31. Zhao F, Yao X, Sun ML. Preliminary analysis of the destructive effect of rain on the Ming dynasty great wall in Yuyang borough, Yulin, Shaanxi Province. Sci Conserv Archaeol. 2014;26(1):1–7 (**in Chinese**).
32. Yao X. Analysis of rainfall erosion models for a typical site of the Ming Great Wall in Yuyang District. Sci Conserv Archaeol. 2018;30(6):82–9 (**in Chinese**).
33. Du YM, Chen WW, Cui K, Zhang KW. Study on damage assessment of earthen sites of the Ming Great Wall in Qinghai Province based on Fuzzy-AHP and AHP-TOPSIS. Int J Architectural Heritage. 2020;14(6):903–16.
34. Richards J, Mayaud J, Zhan HT, Wu FS, Bailey R, Viles H. Modelling the risk of deterioration at earthen heritage sites in drylands. Earth Surf Proc Land. 2020;45(11):2401–16.
35. Yu L, Zhang X, Gao XT, Chen SY, Gu X. Temperature response characteristics of crack deformation of typical earthen sites in Jiayuguan. China Earthquake Eng J. 2020;42(3):751–8 (**in Chinese**).
36. Zhang HY, Yan GS, Zhao TY, Wang XD, Zhang YX. Durability of earthen architecture ruins under cyclic wetting and drying. Rock Soil Mech. 2011;32(2):345–55 (**in Chinese**).
37. Yan GS, Zhang HY, Wang XD, Yang B, Li M. Durability of earthen architecture ruins under cyclic freezing and thawing. Rock Soil Mech. 2011;32(8):2267–73 (**in Chinese**).
38. Yang QY, Li CW. Research on the impact of drying and wetting cycle of capillary water on weathering of soil sites. Chin J Undergr Space Eng. 2012;8(3):517–25 (**in Chinese**).
39. Cui K, Chen WW, Shen YX, Wang XD, Han WF. Experimental study on response of intensity on earthen ruin's soil undergoing recombination process of salinized and dry-wet in arid and semi-arid regions. J Cent South Univ (Sci Technol). 2012;43(11):4451–6 (**in Chinese**).
40. Chen WW, Jia BB, Cai T, Chen HX, Li X. Freeze-thaw deterioration of saline earthen sites under snowmelt or rainfall infiltration. Chin J Geotech Eng. 2022;44(2):334–42 (**in Chinese**).
41. Qu JJ, Cheng GD, Zhang KC, Wang JC, Zu RP, Fang HY. An experimental study of the mechanisms of freeze/thaw and wind erosion of ancient adobe buildings in northwest China. Bull Eng Geol Env. 2007;66(2):153–9.
42. Cui K, Wu GP, Du YM, An XY, Wang ZL. The coupling effects of freeze-thaw cycles and salinization due to snowfall on the rammed earth used in historical freeze-thaw cycles relics in northwest China. Cold Reg Sci Technol. 2019;160:288–99.
43. Richards J, Guo QL, Viles H, Wang YW, Zhang B, Zhang H. Moisture content and material density affects severity of frost damage in earthen heritage. Sci Total Environ. 2022;819:153047.
44. Chen WW, Chen HX, Jia BB, Bi J, Li X. Study of salt migration on the upper part of the great wall under the rainfall-radiation cycle. Bull Eng Geol Env. 2022;81:419.
45. Pu TB, Chen WW, Du YM, Li WJ, Su N. Snowfall-related deterioration behavior of the Ming Great Wall in the eastern Qinghai-Tibet Plateau. Nat Hazards. 2016;84(3):1539–50.
46. Shen YX, Chen WW, Kuang J, Du WF. Effects of salts on earthen materials deterioration after humidity cycling. J Cent South Univ. 2017;24(4):796–806.
47. Cui K, Chong XC, Chen WW, Guan XP, Chen MM. Different effects of shady and sunny slopes in undercutting area of linear earthen ruin in the Hexi Corridor. J Eng Geol. 2017;25(2):547–55.
48. Chen WW, Xia YY, Lei H, Cai T. Evaluation of the degradation effects of earthen sites at constant wind speed based on gray correlation

degree and analytic hierarchy process. J Lanzhou Univ (Nat Sci). 2021;57(3):311–7.
49. Zhang HY, Zhang XC, Chen XN. Research on thermal parameters of different earthen monument soils. Rock Soil Mech. 2014;35(Supp 1):57–62 (**in Chinese**).
50. Zhang HY, Yang L, Liu P, Chen Y, Zhang GC. Study on thermal deterioration simulation test of superficial layer on rammed earthen ruins. J Hunan Univ (Nat Sci). 2018;45(3):149–56 (**in Chinese**).
51. He X, Xu MG, Zhang H, Zhang BJ, Su BM. An exploratory study of the deterioration mechanism of ancient wall-paintings based on thermal and moisture expansion property analysis. J Archaeol Sci. 2014;42:194–200.
52. Chen GQ, Yu ZR. Test for blister and soluble salt in powdering and the layer of plaster for the wall-painting in Cave 351 at Mogao Grottoes. Dunhuang Res. 2008;6:39–45 (**in Chinese**).
53. Wang YJ, Yu QL, Yan M, Ma LY. Research on the mobility of soluble salts for north temple murals. Sci Conserv Archaeol. 2010;22(3):15–20 (**in Chinese**).
54. Zhang D, Zhang SX, Xia Y, Zhang JG, Sun ZC, Fu QL, Hu DD. Preliminary research on water and salt migration at the acrobat pit site in Emperor Qinshihuang's Mausoleum using soil columns. Sci Conserv Archaeol. 2015;27(supp):56–63 (**in Chinese**).
55. Zhang HY, Jiang X, Wang JF, Li XX. A study on the mechanism of capillary-driven transport of soluble salt in mural plaster. Rock Soil Mech. 2016;37(1):1–11 (**in Chinese**).
56. Jin ZL, Hao XQ, Chen GQ, Xia Y, Qian L, Hu HY, Su BM, Zhou T, Lu GX. Simulation study on the migration rate of sodium sulfates and sodium chlorides in soil cultural relics body. Chin J Nat. 2016;38(1):33–8 (**in Chinese**).
57. Jia BB, Chen WW, Chen HX, Li X, Bi J. Effects of snowmelt and rainfall infiltration on the water and salt migration of earthen sites during freeze-thaw process. Int J Architectural Heritage. 2021. https://doi.org/10.1080/15583058.2021.1950234.
58. Jia QQ, Chen WW, Tong YM, Guo QL. Experimental study on capillary migration of water and salt in wall paining plaster: a case study at Mogao Grottoes. China Int J Architectural Heritage. 2022;16(5):705–16.
59. Jin ZL, Chen GQ, Qian L, Su BM, Lu GX. Study on the mechanism of salt damages on the mural paintings of Mogao Grottoes. Chem Res Appl. 2009;21(4):450–4 (**in Chinese**).
60. Lu GX, Zhang SX, Qian L, Xian Y, Hu HY, Rong B, Zhou T. The characteristics of the main dissolved salt and the desalination experiments in Terra-Cotta Warriors and Horses of Emperor Qin Shihuang Mausolesum Site. Chin J Nat. 2015;37(5):341–7 (**in Chinese**).
61. Jin ZL, Chen GQ, Xia Y, Su BM, Zhou T, Lu GX. Comparative study of salt damage caused by sulfates and chlorides to mural paintings – evidence of superpenetration, migration and crystallization destruction resulting from sodium sulfate. Sci Conserv Archaeol. 2015;27(1):29–38 (**in Chinese**).
62. Jin ZL, Chen GQ, Xia Y, Hu HY, Rong B, Xia YN, Zhang SX, Su BM, Zhou T, Lu GX. Sodium sulfate behind earthen relics salt damages: from micro to macro. Sci Conserv Archaeol. 2016;28(1):54–62 (**in Chinese**).
63. Zhang LS, Chen JC, He SY. A summary of the research on the cause and control of salt damage at earthen sites. Dunhuang Res. 2020;3:129–36 (**in Chinese**).
64. Mao WJ, Shen YX, Zhu YP, Bai YF, Sun ML. Disentangling the deformation process of earthen sites and understanding the role of Na2SO4 and precipitation: a case study on the great wall relics of the Ming Dynasty in Yulin China. Stud Conserv. 2021;66(1):51–63.
65. Fredlund DG. Unsaturated soil mechanics in engineering practice. J Geotech Geoenviron Eng. 2006;132(3):286–321.
66. Rahardjo H, Kim Y, Satyanaga A. Role of unsaturated soil mechanics in geotechnical engineering. Int J Geo-Eng. 2019;10(1):8.
67. Zhao TY, Zhang HY, Yan GS, Liu P, Zhang YX. The soil–water characteristics of base coat in Mogao Grottoes Murals. Dunhuang Res. 2011;6:36–42 (**in Chinese**).
68. Shen YX, Chen WW, Bi J, Liu W. Applicability of the MK model to predict the soil–water characteristic curve in consideration of salinity variation. J Lanzhou Univ Nat Sci. 2018;54(1):20–5 (**in Chinese**).
69. Chen WW, Jia QQ, Tong YM. Measurement and curve fitting for soil-water characteristic curve of mural plaster at Mogao Grottoes. Rock Soil Mech. 2020;41(5):1483–91 (**in Chinese**).
70. Li FJ, Wang XD, Guo QL. Adsorbed moisture feature and suction variation characteristics of earthen plaster in Mogao Grottoes under influence of humidity. J Eng Geol. 2021;29(4):1188–98 (**in Chinese**).
71. Li ZX, Wang XD, Sun ML, Chen WW, Guo QL, Zhang HY. Conservation of Jiaohe ancient earthen site in China. J Rock Mech Geotech Eng. 2011;3(3):270–81.
72. Li ZX, Wang XD, Sun ML. Research on consolidation techniques for conserving the ancient city of Jiaohe. Beijing: Science Press; 2008. (**in Chinese**).
73. Chen L, Wang GC, Hu FS, Wang YJ, Liu L. Groundwater hydrochemistry and isotope geochemistry in the Turpan Basin, northwestern China. J Arid Land. 2014;6(4):378–88.
74. Sun ML, Wang XD, Li ZX. Issues concerning earthen sites in northwest China. J Lanzhou Univ (Nat Sci). 2010;46(6):41–5 (**in Chinese**).
75. Sun ML, Li ZX, Wang XD, Wang J. The characteristic of primary damages about the ruins of the Ancient City Jiaohe. Dunhuang Res. 2005;5:92–4 (**in Chinese**).
76. Cui K, Zhang YH, Chen WW, Zhu MJ. Characteristic and formation mechanism of the binary structure in scaling off the surface of rammed earth ruins in arid areas. J Lanzhou Univ Nat Sci. 2019;55(5):647–54 (**in Chinese**).
77. Cui K, Du YM, Zhang YH, Wu GP, Yu L. An evaluation system for the development of scaling off at earthen sites in arid areas in NW China. Heritage Sci. 2019;7:14.
78. Zhang Y, Ye WM, Chen B, Chen YG, Ye B. Desiccation of NaCl-contaminated soil of earthen heritages in the Site of Yar City, northwest China. Appl Clay Sci. 2016;124–125:1–10.
79. Liu P, Zhang HY, Yan GS, Zhao TY, Wang XD. Determination of soil shrinkage characteristic curve of surface soil on ancient earthen architectures. Chin J Rock Mechan Eng. 2010;29(4):842–9 (**in Chinese**).
80. Zhang Y, Ye WM, Chen YG, Chen B. Impact of NaCl on drying shrinkage behavior of low-plasticity soil in earthen heritages. Can Geotech J. 2017;54:1762–74.
81. Zhang Y, Ye WM, Wang Q, Tarantino A. Suction measurement and SWRC modelling for reconstituted salt-laden soils in earthen heritages. Chin J Geotech Eng. 2019;41(9):1661–9 (**in Chinese**).
82. Zhang Y, Ye WM. Water retention characteristics of earthen heritage soil during desiccation considering volumetric change. Chin J Geotech Eng. 2022;44(3):456–63 (**in Chinese**).
83. Zhang Y. Experimental investigation on water-salt coupled mechanism of surface crust and cracking on earthen heritages in arid regions. Doctor thesis. Shanghai: Tongji University; 2018.
84. Hu P, Yang Q, Li PY. Direct and indirect measurement of soil suction in the laboratory. Electron J Geotech Eng. 2010;15(3):1–14.
85. Liu C, Tang CS, Shi B, Suo WB. Automatic quantification of crack patterns by image processing. Comput Geosci. 2013;57:77–80.
86. Peng X, Horn R. Identifying six types of soil shrinkage curves from a large set of experimental data. Soil Sci Soc Am J. 2013;77(2):372–81.
87. Salager S, Nuth M, Ferrari A, Laloui L. Investigation into water retention behaviour of deformable soils. Can Geotech J. 2013;50(2):200–8.
88. Mbonimpa M, Aubertin M, Bussière B, Maqsoud A. A new equation for the suction induced shrinkage of clayey soils. In Proceedings of the 58th Canadian Geotechnical Conference and 6th Joint IAH-CNC and CGS Groundwater Specialty Conference, Saskatoon, Sask. 2005, Paper GS557. [CD-ROM]
89. Tang CS, Shi B, Liu C, Suo WB, Gao L. Experimental characterization of shrinkage and desiccation cracking in thin clay layer. Appl Clay Sci. 2011;52(1–2):69–77.
90. Umezaki T, Kawamura T. Shrinkage and desaturation properties during desiccation of reconstituted cohesive soil. Soils Found. 2013;53(1):47–63.
91. de Carteret R, Buzzi O, Fityus S, Liu XF. Effect of naturally occurring salts on tensile and shear strength of sealed granular road pavements. J Mater Civ Eng. 2014;26(6):04014010.
92. Liu P. Desiccation and cracking on the surface of ancient earthen architectures Doctor thesis. Lanzhou: Lanzhou University; 2009.
93. Trabelsi H, Romero E, Jamei M. Tensile strength during drying of remoulded and compacted clay: the role of fabric and water retention. Appl Clay Sci. 2018;162:57–68.

94. Vaezi AR, Ahmadi M, Cerda A. Contribution of raindrop impact to the change of soil physical properties and water erosion under semi-arid rainfalls. Sci Total Environ. 2017;583:382–92.
95. Vermang J, Demeyer V, Cornelis WM, Gabriels D. Aggregate stability and erosion response to antecedent water content of a loess soil. Soil Sci Soc Am J. 2009;73(3):718–26.
96. Liu P, Zhang HY, Wang JF, Yan GS. Summary of influencing factors of soil surface crust or seal. Arid Land Geography. 2009;32(5):662–8 (**in Chinese**).
97. Wang S, Gao H, Zhao D, Huang SP, Li HR. Effect of rainfall duration on the properties of the soil crust. Sci Conserv Archaeol. 2017;29(6):18–23 (**in Chinese**).
98. Krisdani H, Rahardjo H, Leong EC. Effects of different drying rates on shrinkage characteristics of a residual soil and soil mixtures. Eng Geol. 2008;120(1–2):31–7.
99. Tang CS, Zhu C, Cheng Q, Zeng H, Xu JJ, Tian BG, Shi B. Desiccation cracking of soils: a review of investigation approaches, underlying mechanisms, and influencing factors. Earth Sci Rev. 2021;216:103586.
100. Uday KV, Singh DN. Investigation on cracking characteristics of fine-grained soils under varied environmental conditions. Drying Technol. 2013;31(11):1255–66.
101. Tollenaar RN, van Paassen LA, Jommi C. Observations on the desiccation and cracking of clay layers. Eng Geol. 2017;230:23–31.

Publisher's Note